Journal of Solid State Chemistry 182 (2009) 102–106

Contents lists available at ScienceDirect

Journal of Solid State Chemistry

journal homepage: www.elsevier.com/locate/jssc

# New indium selenite-oxalate and indium oxalate with two- and three-dimensional structures

Jun-Jun Cao [a,b], Guo-Dong Li [a], Jie-Sheng Chen [a,b,*]

[a] State Key Laboratory of Inorganic Synthesis and Preparative Chemistry, College of Chemistry, Jilin University, Changchun 130012, PR China
[b] School of Chemistry and Chemical Engineering, Shanghai Jiao Tong University, Shanghai 200240, PR China

ARTICLE INFO

*Article history:*
Received 10 July 2008
Received in revised form
9 September 2008
Accepted 21 September 2008
Available online 15 October 2008

*Keywords:*
Hydrothermal synthesis
Extended structures
Indium
Selenite-oxalate
Oxalate
Crystal structure

ABSTRACT

Two new indium(III) compounds with extended structures, $[In_2(SeO_3)_2(C_2O_4)(H_2O)_2]\cdot 2H_2O$ (**I**) and $[NH_3(CH_2)_2NH_3][In(C_2O_4)_2]_2\cdot 5H_2O$ (**II**), have been prepared under mild hydrothermal conditions and structurally characterized by single-crystal X-ray diffraction, thermogravimetric analysis and infrared spectroscopy. Compound **I** crystallizes in the triclinic system, space group *P*-1, with $a = 5.2596(11)$ Å, $b = 6.8649(14)$ Å, $c = 9.3289(19)$ Å, $\alpha = 101.78(3)^\circ$, $\beta = 102.03(3)^\circ$, $\gamma = 104.52(3)^\circ$, while compound **II** crystallizes in the orthorhombic system, space group *Fdd*2, with $a = 15.856(3)$ Å, $b = 31.183(6)$ Å, $c = 8.6688(17)$ Å. In compound **I**, indium-selenite chains are bridged by oxalate units to form two-dimensional (2D) $In_2(SeO_3)_2C_2O_4$ layers, separated by non-coordinating water molecules. In compound **II**, the indium atoms are connected through the oxalate units to generate a 3D open framework containing cross-linked 12- and 8-membered channels.

## 1. Introduction

Inorganic–organic hybrid materials have attracted considerable attention due to their interesting structural topologies and potential applications in the areas of catalysis, sorption, separation processes, and device manufacture [1–3]. Among the hybrid compounds are metal oxalates which exhibit vast diversity and unusual features in structure [4,5]. Oxalate anion displays various coordination modes when it is bound to metal cations. For example, as a bridging ligand, the oxalate may lead to open-framework structures with varying dimensionality, whereas as a bischelate ligand, it may bring interesting magnetic properties to the corresponding compounds due to their relatively short bonds between metal centers. A variety of metal oxalates with 1D, 2D and 3D structures have been reported during the past two decades [6–13].

The incorporation of the oxalate group in metal-oxo open-frameworks is also of interest because additional structure features may appear after the oxalate incorporation [14–17]. In the framework of these compounds, the oxalate unit can act either as a ligand or as a bridging species. Most of oxalate-incorporated metal-oxo framework compounds have been focused on metal phosphates [15–17], while less attention has been paid to metal selenites despite their potential applications in such fields as second harmonic generation (SHG) [18]. Up to date, only a few examples of metal selenite-oxalates have appeared in the literature [19,20]. In addition, the stereochemically active lone pair of Se(IV) ion affect the coordination geometry and the structures of the metal selenite-oxalate compounds to a great extent. Therefore, it is of importance to obtain more metal selenite-oxalate compounds and to elucidate their structure features.

On the other hand, although the group 13 metals (Al, Ga, In) have been widely used in the preparation of zeolites and metal-phosphates [21–23], the synthesis of other open framework structures involving these metals is rather limited [24–26]. In this paper, we report the synthesis and structure characterization of a new layered indium selenite-oxalate $[In_2(SeO_3)_2(C_2O_4)(H_2O)_2]\cdot 2H_2O$ (**I**) and a unique amine-templated 3D indium oxalate open-framework $[NH_3(CH_2)_2NH_3][In(C_2O_4)_2]_2\cdot 5H_2O$ (**II**).

## 2. Experimental section

### 2.1. Materials and methods

$In(NO_3)_3\cdot 6H_2O$, $SeO_2$, $H_2SeO_4$ (40% aqueous solution) were purchased from Shanghai Chemical Reagent Company, and oxalic acid, ethylenediamine (en) and other reagents from Beijing

---

[*] Corresponding author at: School of Chemistry and Chemical Engineering, Shanghai Jiao Tong University, Shanghai 200240, PR China. Fax: +86 21 54741297.
*E-mail address:* chemcj@sjtu.edu.cn (J.-S. Chen).

0022-4596/$ - see front matter © 2008 Elsevier Inc. All rights reserved.
doi:10.1016/j.jssc.2008.09.023

Chemical Reagent Company. All of the reagents were of analytical grade and used as received. Deionized water was used in all the experiments.

The IR spectra were recorded within the 400–4000 $cm^{-1}$ region on a Bruker IFS 66V/S Fourier transform infrared (FT-IR) spectrometer using KBr pellets. The C, H, and N elemental analysis was conducted on a Perkin-Elmer 240C element analyzer, whereas the inductively coupled plasma (ICP) analysis was performed on a Perkin-Elmer Optima 3300DV ICP spectrometer. The powder X-ray diffraction (XRD) data were collected on a Rigaku D/Max 2550 diffractometer with Cu*K*α radiation ($\lambda = 1.5418$ Å), and the recording speed was 24°/min over the $2\theta$ range of 4–40° at room temperature. The simulated and experimental powder XRD patterns of compounds **I** and **II** are shown in the supplemental data (Fig. S1). The thermogravimetric (TG) and differential thermal analysis (DTA) were performed on a Netzsch STA 449C thermogravimetric analyzer under an atmospheric environment at a heating rate of 20 °C/min.

### 2.2. *Synthesis of compounds **I** and **II***

$In_2(SeO_3)_2C_2O_4 \cdot 4H_2O$ (**I**). A mixture of $In(NO_3)_3 \cdot 6H_2O$ (96 mg, 0.25 mmol) and $SeO_2$ (28 mg, 0.25 mmol) in 9 mL of distilled water were stirred for 10 min followed by addition of the oxalic acid (32 mg, 0.5 mmol). After stirring for another 30 min, the resultant mixture was sealed into an autoclave equipped with a Teflon liner (15 mL) and heated at 140 °C for 3 days. The autoclave was then cooled at 10 °C/h to room temperature. Colorless plate-shaped crystals of **I** were obtained in 83% yield based on indium. The product consisted of single crystals and no crystals with other shapes were observed, suggesting that the product was phase-pure. The initial and final pH values of the solution did not show appreciable change and were close to 3. Elemental and ICP analysis results for compound **I**, $C_2H_8In_2O_{14}Se_2$: In, 35.75; Se, 25.45; C, 3.88; H, 1.43%. Calcd.: In, 35.68; Se, 24.54; C, 3.73; H, 1.25%.

$[NH_3(CH_2)_2NH_3][In(C_2O_4)_2]_2 \cdot 5H_2O$ (**II**). A mixture of $In(NO_3)_3 \cdot 6H_2O$ (96 mg, 0.25 mmol), oxalic acid (40 mg, 0.625 mmol), $H_2SeO_4$ (0.17 mL, 0.103 mmol) and 36% HCl (0.1 mL) in 9 mL of distilled water were stirred for 30 min. After 0.025 mL ethylenediamine (0.375 mmol) was added, the mixture was sealed into an autoclave equipped with a Teflon liner (15 mL) and heated at 120 °C for 3 days. The autoclave was then cooled at 10 °C/h to room temperature. Colorless octahedral single crystals of **II** were obtained in 56% yield based on indium. No crystals with a morphology other than octahedron were present in the product, indicating the phase purity of the as-synthesized material. The initial and final pH values of the solution did not show appreciable change and were close to 2. Elemental and ICP analysis results for compound **II**, $C_{10}H_{20}In_2N_2O_{21}$: In, 29.89; C, 16.54; H, 1.21; N, 3.64%. Calcd.: In, 31.29; C, 16.37; H, 2.75; N, 3.82%.

### 2.3. *Determination of crystal structure*

Crystallographic data of compound **I** were collected on a Rigaku RAXIS-RAPID single-crystal diffractometer equipped with a narrow-focus, 5.4-kW sealed-tube X-ray source (graphite-monochromated Mo*K*α radiation with $\lambda = 0.71073$ Å) at a temperature of $20 \pm 2$ °C. The data processing was accomplished with the PROCESS-AUTO processing program. Crystallographic data for **II** were recorded at room temperature on a Bruker-AXS Smart CCD diffractometer equipped with a normal-focus, 2.4-kW X-ray source (graphite-monochromated Mo*K*α radiation with $\lambda = 0.71073$ Å) operating at 50 kV and 40 mA with increasing $\omega$ (width of 0.3° and exposure time of 30 s/frame). Both of the structures were solved by direct methods using the program SHELXS-97 [27] and refined by full-matrix least-squares techniques against $F^2$ using the SHELXTL-97 [28] crystallographic software package. Non-hydrogen atoms were refined with anisotropic temperature parameters, and hydrogen atoms of the ligands were refined as rigid groups. The hydrogen atoms associated with the water molecules of compound **II** were not located from the difference Fourier maps. The detailed crystallographic data and structure refinement parameters for **I** and **II** are summarized in Table 1. The final atomic coordinates and

**Table 1**
Crystal data and structure refinement parameters for compounds **I** and **II**

| Compound | **I** | **II** |
|---|---|---|
| Empirical formula | $CH_4InO_7Se$ | $C_{40}H_{64}In_8N_8O_{80}$ |
| Space group | *P*-1 | *Fdd*2 |
| *a* (Å) | 5.2596 (11) | 15.856 (3) |
| *b* (Å) | 6.8649 (14) | 31.183 (6) |
| *c* (Å) | 9.3289 (19) | 8.6688 (17) |
| α (°) | 101.78 (3) | 90.00 |
| β (°) | 102.03 (3) | 90.00 |
| γ (°) | 104.52 (3) | 90.00 |
| *Z* | 2 | 2 |
| Formula mass | 321.82 | 2855.55 |
| $\rho_{calc}$ (g/cm$^3$) | 3.481 | 2.213 |
| $\mu$ (mm$^{-1}$) | 9.760 | 2.254 |
| $\theta$ range (°) | 3.18–27.47 | 3.32–27.44 |
| Index ranges | $-6 <= h <= 6$, $-8 <= k <= 8$, $-12 <= l <= 10$ | $-20 <= h <= 20$, $-40 <= k <= 40$, $-11 <= l <= 9$ |
| Refinement method | Full-matrix least-squares on $\lvert F^2 \rvert$ | Full-matrix least-squares on $\lvert F^2 \rvert$ |
| Crystal size (mm) | 0.30 × 0.30 × 0.15 | 0.50 × 0.26 × 0.21 |
| *R* indices [$I > 2\sigma(I)$] | $R_1 = 0.0311$, $wR_2 = 0.0714$ | $R_1 = 0.0191$, $wR_2 = 0.0420$ |
| *R* indices (all data) | $R_1 = 0.0355$, $wR_2 = 0.0787$ | $R_1 = 0.0195$, $wR_2 = 0.0421$ |
| GOF on $F^2$ | 1.076 | 1.161 |
| *F*(000) | 298 | 2784 |
| Observed data [$I > 2\sigma(I)$] | 1233 | 2187 |
| Reflections collected | 3025 | 9968 |
| Independent reflections | 1393 [*R*(int) = 0.0450] | 2225 [*R*(int) = 0.0243] |
| Data/restraints/parameters | 1393/0/105 | 2225/1/159 |

$R_1 = \sum ||F_0| - |F_c|| / \sum |F_0|$.
$wR_2 = \{\sum[w(F_0^2 - F_c^2)^2] / \sum[w(F_0^2)]^2\}^{1/2}$.

selected bond distances are presented in Tables S1 and S3 for **I**, and Tables S2 and S3 for **II**.

CCDC nos. 694020 (**I**) and 694021 (**II**) contain the supplementary crystallographic data for this paper. These data can be obtained free of charge from The Cambridge Crystallographic Data Centre via www.ccdc.cam.ac.uk/data_request/cif.

## 3. Results and discussion

### *3.1. Synthesis and initial characterization*

Hydrothermal synthesis, in the presence of organic templating/bonding agents, is a convenient method to prepare novel structural frameworks, such as zeolites and MOFs. In the synthesis of compound **I**, we attempted to use the maleic acid instead of oxalate acid, and **I** was successfully synthesized. Clearly, the oxalate arises from the mild decomposition of maleic acid in the hydrothermal environment. The slow release of oxalate results in the formation of high quality crystals. The formation of **II** is sensitive to the existence of $H_2SeO_4$ and the quantity of $H_2C_2O_4$. In the absence of $H_2SeO_4$ or if the amount of $H_2C_2O_4$ is small, compounds other than **II** form. A synthetic procedure similar to that for **II** has also been adopted previously for the preparation of an indium selenite-oxalate $[H_2en]_{0.5}[In(SeO_4)(C_2O_4)(H_2O)_2]$ [19]. However, it is interesting to note that there is no selenate group in **II**, probably because of the difference in pH value and in molar ratio of the reactants for the two reaction systems. Other inorganic acids instead of selenic acid have also been used for the preparation of **II**, but no crystals of **II** are produced in these cases. It seems that the selenic acid plays a role in the formation of the indium oxalate compound although the selenate group is not involved in the final structure of the compound.

### *3.2. Structure of $[In_2(SeO_3)_2(C_2O_4)(H_2O)_2]\cdot 2H_2O$ (I)*

The structure of compound $[In_2(SeO_3)_2(C_2O_4)(H_2O)_2]\cdot 2H_2O$ (**I**) features an interesting layered structure constructed from $InO_7$ pentagonal bipyramid, $SeO_3^{2-}$ pseudo-tetrahedra and planar $C_2O_4^{2-}$ groups. As shown in Fig. 1, the asymmetric unit of **I** consists of 10 independent non-hydrogen atoms, nine of which, including one In(III) atom, one Se(VI) atom, six O atoms and one C atom, belong to the inorganic framework, and the other one of which is the non-coordinating water molecule located in the space between the adjacent layers. The central In(III) ion is seven-coordinated by one $SeO_3^{2-}$ group in a bidentate fashion, two $SeO_3^{2-}$ groups in unidentate fashions, one oxalate anion in a bidentate chelating fashion and one terminal water molecule. The five oxygen atoms (O1, O3, O4, O5, O1A) from two bidentate $SeO_3^{2-}$, one oxalate and one unidentate $SeO_3^{2-}$ group lie in a plane and form a pentagon, while the other two oxygen atoms (O2, O6) of another unidentate $SeO_3^{2-}$ group and a terminal water form two vertices above and below the pentagon. The adjacent two In atoms are interconnected by two shared selenite oxygen atoms O(1) from different selenites to form $In_2O_4$ binuclear clusters. These dimeric units link each other through two $Se(1)O_3$ pseudo-tetrahedra, resulting in step-like double chains running along the *b*-axis. Interestingly, the infinite chains are further connected by the oxalate anions to yield a layer, where each oxalate anion coordinates to two In(III) centers in a bidentate mode. Each layer consists of 8-membered ring windows formed by the edges of four $InO_7$ decahedra, two selenite pseudo-tetrahedra and two oxalate units (Fig. 2). Adjoining layers are aligned such that straight channels approximately along the [12−1] direction are formed (Fig. 3a). The water molecule coordinated to the In atom is in a direction perpendicular to the plane of the layers and projects into the interlayer space (Fig. 3b). The slight distortion observed for the $InO_7$ decahedra is demonstrated by the wide range of In–O bond lengths [2.106(4)–2.322(4) Å] and the narrow O–In–O angles [64.53(1)–72.68(7)] (Table S3) [16,19], and this distortion is believed to be caused by the chelation of oxalate groups and the bidentate $SeO_3^{2-}$ groups. The In–O distances range from 2.106(4) to 2.322(4) Å, which are comparable to those of the reported indium compounds [19]. The $SeO_3^{2-}$ anion is 3-connected, bridging two In(1) atom, while the oxalate anion is tetradentate, bridging two In atoms as well. The lattice water molecules are located in the voids of the layer, and form an extensive hydrogen-bonding network with O4 of $SeO_3^{2-}$ anions and O6 of oxalate anions (Table S3). Although the hydrogen bonds are cross-linked in each layer, no direct hydrogen bond has been found between adjacent layers (Fig. 3b).

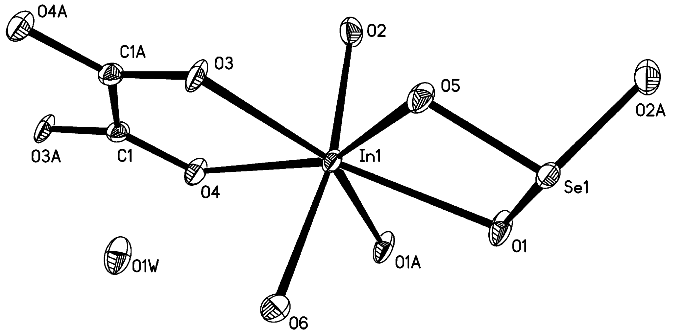

**Fig. 1.** ORTEP drawing of the selected unit of **I**. Thermal ellipsoids are shown at 30% probability.

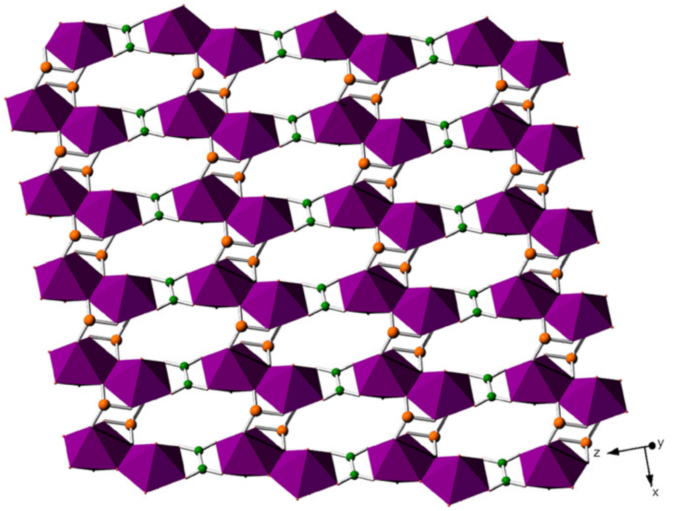

**Fig. 2.** Polyhedral view of an $In_2(SeO_3)_2C_2O_4$ 2D layer in the [010] plane of compound **I**.

### *3.3. Structure of $[NH_3(CH_2)_2NH_3][In(C_2O_4)_2]_2\cdot 5H_2O$ (II)*

The structure of compound **II** features an ordered 3D framework constructed by the indium atoms and the oxalate units. The asymmetric unit of **II**, as depicted in Fig. 4, consists of one In atom, two independent oxalate groups, a $(H_4en)^{2+}$ cation (en = ethylenediamine) and five lattice water molecules. Each In(III) ion binds to eight oxygen atoms from four bidentate oxalate ligands. The $InO_8$ dicapped trigonal prism, with In–O bond lengths ranging between 2.167(3) and 2.422(3) Å (Table S3), is slightly distorted because of the chelation of the oxalate groups. The

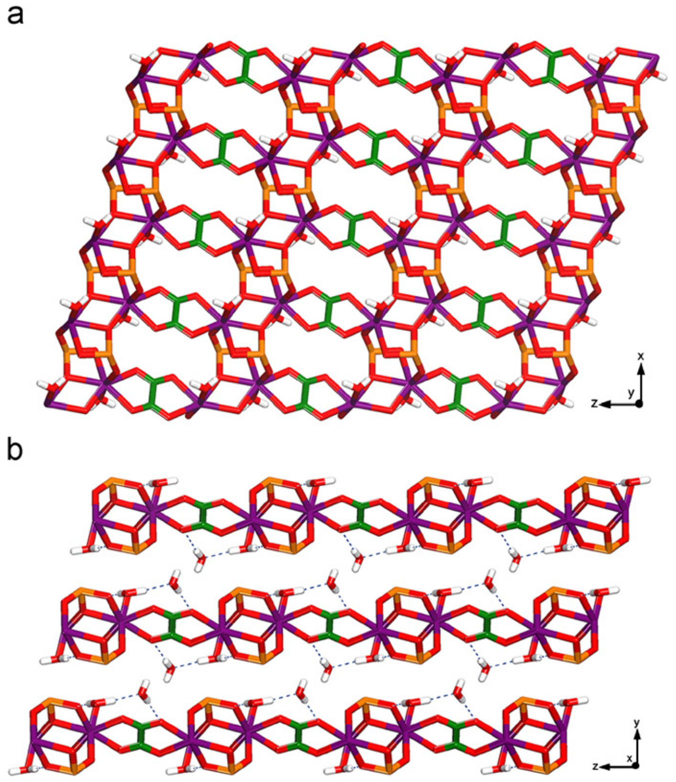

**Fig. 3.** View of the structure of **I** along the [010] direction (a), and along the [100] direction (b). Hydrogen bonds are drawn as dotted lines.

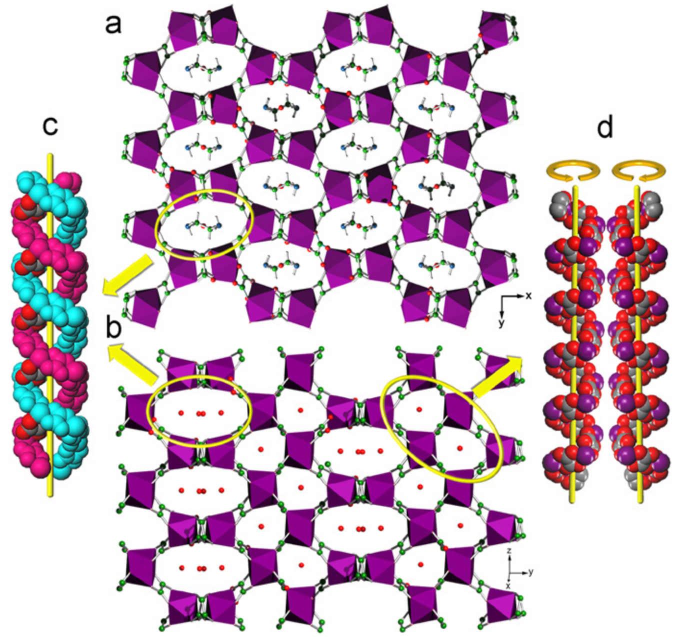

**Fig. 5.** Polyhedral view of the structure of **II** along the [001] direction (a), showing 12-membered channels and the occluded amine molecules, and view of the structure of **II** along the [1003] direction (b), showing 8- and 12-membered channels filled with lattice water. The helical chains, sharing an oxalate unit, form 12-membered channels running along the [001] and [1003] direction (c), and 8-membered channels running along the [1003] direction (d).

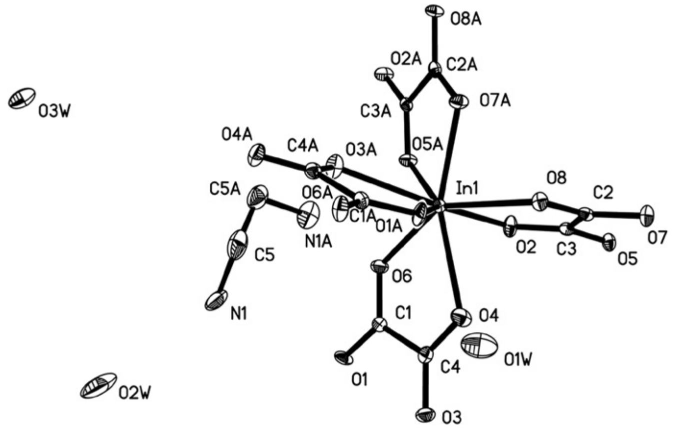

**Fig. 4.** ORTEP drawing of the selected unit of **II**. Thermal ellipsoids are shown at 30% probability.

O–In–O bite angles of the bidentate oxalate ligands with the metal center are 70.04(10)–72.57(9)°. The In–O and O–In–O distances and angles are in the expected ranges [7]. There are two crystallographic oxalate groups, both of which are bischelate ligands. The oxalate groups link $InO_8$ polyhedra to give rise to a 3D framework containing both 8- and 12-membered channels. The $(H_4en)^{2+}$ cations and water molecules O(2w) are located in the 12-membered ring channels along the [001] direction (Fig. 5a). The channels, which have windows linked by six $InO_7$ polyhedra and six oxalate anions, are formed by two helical chains, sharing an oxalate unit and extending along the [001] direction (Fig. 5c). The other two types of channels are in the [1003] direction, filled with the lattice water O(3w) and O(4w), respectively (Fig. 5b). The 8-membered channel is formed by a single helix, and the 12-membered one is similar to the one in [001] direction as shown in Fig. 5d. The ethylenediamine plays an important role in the construction and stabilization of the 3D framework of **II**. In the compound, the en molecules are protonated and interact strongly with the negatively charged oxygen atoms of the oxalate ligands.

The simulated and experimental powder XRD patterns of compounds **I** and **II** are shown in the supplemental data (Fig. S1). The experimental patterns are in good agreement with the corresponding simulated ones, further confirming the phase purity of the as-synthesized products.

Thermogravimetric analyses of **I**, **II** were conducted in flowing air within the temperature range between 35 and 800 °C (Fig. S2). Both compounds show two main weight losses and the XRD indicates that the samples (**I** and **II**) are thermally stable up to 262 and 252 °C, respectively. The first weight losses correspond to the release of the lattice water molecules (for **I**: found 5.62%, calcd. 5.60%; for **II**: found 7.91%, calcd. 7.74%). The coordinating water molecules in compound **I** are not lost at this stage because of their strong bonds with the indium ions. The second weight loss of compound **I** seems complicated, but it can be attributed to the removal of the coordinating water and $SeO_2$. As expected, the final residues are mainly $In_2O_3$ (found 43.23%, calcd. 43.14%) as confirmed by powder XRD. The second weight loss of compound **II** can be divided into two sub-steps. In the range of 252–405 °C, the mass loss corresponds to the decomposition of the protonated ethylenediamine and the oxalate groups. The residue is $In_2(CO_3)_3$ (found 57.55%, calcd. 58.70%) as indicated by the powder XRD pattern. In the range of 405–800 °C, the $In_2(CO_3)_3$ decomposes to the final product $In_2O_3$ (found 40.47%, calcd. 39.78%) [8].

The IR spectra of compounds **I** and **II** are shown in Fig. S3. The three broad bands centered at 3582, 3506 and 2966 $cm^{-1}$ for **I** can be attributed to the symmetric and asymmetric stretching modes of water molecules. Meanwhile, the bands in the region of 3715–3280 $cm^{-1}$ for **II** correspond to the $\upsilon$(N–H) of the amine and $\upsilon(H_2O)$ of the lattice water molecules. The characteristic bonds of oxalate groups are observed distinctly at $1655\,cm^{-1}$ [$\upsilon_{as}(CO_2)$], 1360, $1317\,cm^{-1}$ [$\upsilon_s(CO_2)$], and $795\,cm^{-1}$ [$\delta(CO_2)$] for **I**, while both bands appear at $1635\,cm^{-1}$ [$\upsilon_{as}(CO_2)$] (also $\delta$(NH)), 1508, 1455, 1358, $1211\,cm^{-1}$ [$\upsilon_s(CO_2)$], and $812\,cm^{-1}$ [$\delta(CO_2)$] for **II**. The expected bending mode of water around $1600\,cm^{-1}$ is overlapped by the intense oxalate band. In **I**, the peaks at 712 and $872\,cm^{-1}$ can be assigned to $\upsilon$(Se–O) vibrations in $SeO_3^{2-}$, and the bands found at 534, 490, $434\,cm^{-1}$ can be attributed to $\delta(SeO_3)$ and $\delta$(In–O) [20]. Compared with **I**, the bending vibration mode of In–O is observed at 488 and $436\,cm^{-1}$ for **II**. The extra bands at 1184, 1061, 980, $930\,cm^{-1}$ for **II** are ascribed to $\upsilon$(C–N) and $\delta$(NH) of the ethylenediamine [16].

## 4. Conclusions

Two new indium compounds have been successfully prepared under hydrothermal conditions. $[In_2(SeO_3)_2(C_2O_4)(H_2O)_2]\cdot 2H_2O$ (**I**) features an interesting layered structure constructed by indium polyhedra, selenite anions and oxalate groups. The incorporation of the oxalate group in indium selenite network enriches the coordination geometry and structure of the metal selenite compounds. The compound $[NH_3(CH_2)_2NH_3][In(C_2O_4)_2]_2\cdot 5H_2O$ (**II**), is formed by using ethylenediamine as structure directing agent and displays a 3D open framework with attractive 8- and 12-membered channels along the [001] and [1003] directions. The diversity of coordinated number for indium(III) is demonstrated by the incorporation of oxalate ligand, and our finding suggests the possibility to synthesize more indium hybrid materials with interesting open-framework structures.

## Acknowledgments

This work was supported by the National Natural Science Foundation of China (20731003) and the National Basic Research Program of China (2007CB613303).

## Appendix A. Supporting Information

Supplementary data associated with this article can be found in the online version at doi:10.1016/j.jssc.2008.09.023.

## References

[1] O.M. Yaghi, H. Li, C. Davis, D. Richardson, T.L. Groy, Acc. Chem. Res. 31 (1998) 474–484.
[2] G. Ferey, Chem. Mater. 13 (2001) 3084–3098.
[3] A.K. Cheetham, C.N.R. Rao, R.K. Feller, Chem. Commun. (2006) 4780–4795.
[4] C.N.R. Rao, S. Natarajan, R. Vaidhyanathan, Angew. Chem. Int. Ed. 43 (2004) 1466–1496.
[5] M. Gruselle, C. Train, K. Boubekeur, P. Gredin, N. Ovanesyan, Coord. Chem. Rev. 250 (2006) 2491–2500.
[6] M. Dan, C.N.R. Rao, Angew. Chem. Int. Ed. 45 (2006) 281–285.
[7] E. Jeanneau, N. Audebrand, D. Louer, Chem. Mater. 14 (2002) 1187–1194.
[8] A. Mohanu, C. Brouca-Cabarrecq, J.C. Trombe, J. Solid State Chem. 179 (2006) 3–17.
[9] O.R. Evans, W.B. Lin, Cryst. Growth Des. 1 (2001) 9–11.
[10] Z.X. Chen, Y.M. Zhou, L.H. Weng, H.Y. Zhang, D.Y. Zhao, J. Solid State Chem. 173 (2003) 435–441.
[11] S.H. Yang, G.B. Li, S.J. Tian, F.H. Liao, J.H. Lin, J. Solid State Chem. 178 (2005) 3703–3707.
[12] N. Audebrand, S. Raite, D. Louer, Solid State Sci. 5 (2003) 783–794.
[13] E. Gavilan, N. Audebrand, E. Jeanneau, Solid State Sci. 9 (2007) 985–999.
[14] S. Chakrabarti, S. Natarajan, Angew. Chem. Int. Ed. 41 (2002) 1224–1226.
[15] C.H. Lin, K.H. Lii, Inorg. Chem. 43 (2004) 6403–6407.
[16] M. Mrak, U. Kolitsch, C. Lengauer, V. Kaucic, E. Tillmanns, Inorg. Chem. 42 (2003) 598–604.
[17] S. Natarajan, Angew. Chem. Int. Ed. 41 (2008) 4798–4828.
[18] K.M. Ok, P.S. Halasyamani, Chem. Mater. 14 (2002) 2360–2364.
[19] M.L. Feng, X.L. Li, J.G. Mao, Cryst. Growth Des. 7 (2007) 770–777.
[20] M.L. Feng, H.Y. Ye, J.G. Mao, J. Solid State Chem. 180 (2007) 2471–2477.
[21] A.K. Cheetham, G. Ferey, T. Loiseau, Angew. Chem. Int. Ed. 38 (1999) 3268–3292.
[22] J.H. Yu, R.R. Xu, Chem. Soc. Rev. 35 (2006) 593–604.
[23] C. Chen, Y.L. Liu, S.H. Wang, G.H. Li, M.H. Bi, Z. Yi, W.Q. Pang, Chem. Mater. 18 (2006) 2950–2958.
[24] W.H. Casey, M.M. Olmstead, B.L. Phillips, Inorg. Chem. 44 (2005) 4888–4890.
[25] S.H. Luo, Y.C. Jiang, S.L. Wang, H.M. Kao, K.H. Lii, Inorg. Chem. 40 (2001) 5381–5384.
[26] Z.Z. Lin, F.L. Jiang, L. Chen, C.Y. Yue, D.Q. Yuan, A.J. Lan, M.C. Hong, Cryst. Growth Des. 7 (2007) 1712–1715.
[27] G.M. Sheldrick, SHELXS-97, Programs for X-Ray Crystal Structure Solution, University of Göttingen, Göttingen, Germany, 1997.
[28] G.M. Sheldrick, SHELXL-97, Programs for X-Ray Crystal Structure Refinement, University of Göttingen, Göttingen, Germany, 1997.